



**HAL**  
open science

## Stability to oxidation and interfacial behavior at the air/water interface of minimally-processed versus processed walnut oil-bodies

Jeanne Kergomard, Gilles Paboeuf, Nathalie Barouh, Pierre Villeneuve, Olivier Schafer, Tim Wooster, Claire Bourlieu-Lacanal, V. Vié

### ► To cite this version:

Jeanne Kergomard, Gilles Paboeuf, Nathalie Barouh, Pierre Villeneuve, Olivier Schafer, et al.. Stability to oxidation and interfacial behavior at the air/water interface of minimally-processed versus processed walnut oil-bodies. *Food Chemistry*, 2021, 360, pp.129880. 10.1016/j.foodchem.2021.129880 . hal-03224107

**HAL Id: hal-03224107**

**<https://hal.science/hal-03224107>**

Submitted on 14 Jun 2021

**HAL** is a multi-disciplinary open access archive for the deposit and dissemination of scientific research documents, whether they are published or not. The documents may come from teaching and research institutions in France or abroad, or from public or private research centers.

L'archive ouverte pluridisciplinaire **HAL**, est destinée au dépôt et à la diffusion de documents scientifiques de niveau recherche, publiés ou non, émanant des établissements d'enseignement et de recherche français ou étrangers, des laboratoires publics ou privés.

**Title:** Stability to oxidation and interfacial behavior at the air/water interface of minimally-processed versus processed walnut oil-bodies

**Name(s) of Author(s)** Jeanne Kergomard<sup>1,2,3</sup>, Gilles Paboeuf<sup>1,4</sup>, Nathalie Barouh<sup>3</sup>, Pierre Villeneuve<sup>3</sup>, Olivier Schafer<sup>5</sup>, Tim J. Wooster<sup>5</sup>, Claire Bourlieu<sup>2</sup>, Véronique Vié<sup>1,4\*</sup>

**Author Affiliation(s)** <sup>1</sup> IPR Institute of Physics, UMR UR1 CNRS 5261, Rennes 1 University, France; <sup>2</sup> IATE, Univ Montpellier, INRAE, Institut Agro, Montpellier, France; <sup>3</sup> QUALISUD, Univ Montpellier, CIRAD, Institut Agro, IRD, Univ Réunion, Montpellier, France; <sup>4</sup> Univ Rennes 1, CNRS, ScanMAT – UMS 2001 F-35042 Rennes, France; <sup>5</sup> Institute of Materials Science, Nestlé Research, Lausanne, Switzerland

**\*Corresponding author:** Dr. Véronique Vié, Institut de Physique de Rennes, Campus de Beaulieu, UMR UR1 CNRS 5261, Université de Rennes 1, 35042 Rennes cedex, phone number: 033223235645 and E-mail address : veronique.vie@univ-rennes1.fr

**Present/permanent address:** Institut de Physique de Rennes, campus de Beaulieu, 35042 Rennes cedex – France

**Word count:** 6684

**Total number of tables/figures:** 6

**Abbreviations**

AFM: Atomic force microscopy

ALA:  $\alpha$ -linolenic acid

BAM: Brewster angle microscopy

BuOH: Butanol

CLSM: Confocal laser scanning microscopy

DELTA: Ellipsometric angle

DAG: Diacylglycerol

EggPC: Phosphatidylcholine from egg yolk

EggPC-WOIL: model solution containing EggPC (2% wt) and WOIL (95% wt) diluted at 4% wt

EtOH: Ethanol

FA: Fatty acid

FAME: Fatty acid methyl ester

FFA: Free fatty acid

He-Ne: Helium-neon

HHP: High-pressure homogenization

HHPT: High-pressure homogenization following by a heat treatment

HNO<sub>3</sub>: Nitric acid

HPLC: High performance liquid chromatography

LA: Linoleic acid

MAG: Monoacylglycerol

MDA: Malondialdehyde

MeOH: Methanol

MP: Minimally processed

NaCl: Sodium chloride

OB: Oil body

Oleo-TAG: model solution containing oleosins (3% wt) and TAG (95% wt) diluted at 4% wt

Oleo-WOIL: model solution containing oleosins (3% wt) and WOIL (95% wt) diluted at 4% wt

PI: Surface pressure

pH: Potential hydrogen

PC: Phosphatidylcholine

PE: Phosphatidylethanolamine

PI: Phosphatidylinositol

pI: Isoelectric point

PL: Phospholipid

PS: Phosphatidylserine

PUFA: Polyunsaturated fatty acids

PV: Peroxide value

QNM: Quantitative nanomechanic

Rd-DOPE: 1,2-dipalmitoyl-sn-glycero-3-phosphoethanolamin-N-(lissamin rhodamin B sulfonyl)

TAG: Triacylglycerol

TBA: Thiobarbituric acid

TBARS: Thiobarbituric acid reactive substances

TCA: Trichloroacetic acid

TLC: Thin-layer chromatography

Tris-HCl: tris(hydroxymethyl)aminomethane hydrochloride

UP: Ultrapure (water)

WOIL: Commercial walnut oil

**ABSTRACT** Oil bodies (OB), the form of triacylglycerol storage in seeds, are interesting natural assemblies for nutritional applications. In walnuts, OB contain an important amount of polyunsaturated fatty acids that could be interesting food ingredients but may be prone to oxidation. The oxidative and interfacial behavior of walnut OB, either minimally-processed or after processing, were compared with processed complex walnut juice. The good oxidative stability of minimally-processed OB over 10 days ( $PV \leq 8.4$  meq  $O_2/kg$ , TBARS=1.4 mmol eq MDA/kg) and of processed walnut complex matrixes over 20 days ( $PV \leq 4.8$  meq  $O_2/kg$ , TBARS=1.4 mmol eq MDA/kg) was evidenced. In comparison, processing of OB promoted their oxidation. The interfacial studies led to the proposition of a new model of adsorption for minimally-processed OB that will be useful to design functional emulsion or foam in which OB act as emulsifiers.

**KEYWORDS:** walnut beverage emulsion; oil bodies; oxidative stability; ellipsometry; minimalist processes

## 1 INTRODUCTION

Oleosomes or oil bodies (OB) are very specific lipoproteic entities that enable plants to store the energy they need for germination and growth (Khor et al., 2013; Walther & Farese, 2012). OB vary in size from nanoscopic (500 nm) to a few micrometers (2.5  $\mu\text{m}$ ) (Frandsen et al., 2001). The structure of an OB is based on a triacylglycerol (TAG) core droplet (94-98% wt.) surrounded by a monolayer of phospholipids (PL) (0.6-2% wt.) with embedded proteins (0.6-3% wt.) (Huang, 1994; Napier et al., 2001). Such lipoproteic monolayer protects the OB from chemical or mechanical stresses (Nikiforidis et al., 2014). Three types of proteins are present in the lipid monolayer, oleosins, caleosins and stereosins; oleosins being the most abundant (1-4% wt.) (Napier et al., 2001). Thanks to the presence of oleosins, OB are remarkably stable against aggregation and coalescence (Barre et al., 2018; Napier et al., 2001; Nikiforidis et al., 2014). This stability is attributed to steric hindrance and to the negatively charged surface of the monolayer at physiological pH, leading to electrostatic repulsion between OB and reducing aggregation (Shimada et al., 2018). The natural stability of these assemblies explains the considerable attention recently paid to OB (Nikiforidis, 2019). In addition, they can be considered as minimally processed entities that deliver TAG, liposoluble vitamins, and proteins for human nutrition. While a multitude of products is derived from nuts and seeds, few exist where the OB remains in its native or minimally-processed form.

Walnuts are among the most widely consumed commercially grown tree nuts in the world (Hayes et al., 2016). Their consumption is associated with many health benefits, including reducing the risk of cardiovascular disease, and neurological disorders (Simopoulos, 2002). These benefits are attributed to their fatty acid (FA) profile, which is rich in polyunsaturated

fatty acids (PUFA) (Hayes et al., 2016). Walnut lipids contain 90% unsaturated FA, of which 12-16% is  $\alpha$ -linolenic acid (ALA, C18:3,  $\omega$ 3) that very likely explain the cardioprotective effects of a diet rich in walnuts (Maguire et al., 2004). Walnut lipids are also considered to be a good source of vitamins and dietary fibers (Miraliakbari & Shahidi, 2008). To date, most research on walnut lipids has focused on their chemical composition (Venkatachalam & Sathe, 2006). In addition to TAG, tree nut lipids contain phytosterols, PL, and tocopherols, which are known to confer good oxidative stability to oil in water emulsion (Samdani et al., 2018).

Several studies have been dedicated to OB colloidal stability, with special emphasis on soybean source (Kapchie et al., 2013; Zhao et al., 2016). The chemical stability during the storage of emulsions prepared with OB from oilseeds has been investigated, including issues of endogenous hydrolytic activity (De Chirico et al., 2020) and oxidative sensitivity (B. Chen et al., 2012). Nevertheless, the use of oilseed OB with high PUFA content is limited because of their susceptibility to oxidation (Nuchi et al., 2002). Lipid oxidation is an undesirable reaction in food applications and the dispersion of lipids in emulsions further increases this phenomenon by increasing contact with oxygen and pro-oxidant species. This explains why lipid oxidation is a major cause of degradation during the manufacture and storage of food products (Villière, 2005), and also explains why the use of OB in beverages requires a good understanding of their physical and chemical stability to obtain a product that meets consumer expectations.

Despite the high number of publications on vegetal juices and OB chemical characterization (Tzen et al., 1993), questions remain open regarding the interfacial behavior of OB. Some insights have been gained into the physical stability of natural OB (White et al., 2008) and their organization at the interface (Bettini et al., 2014; Waschatko et al., 2012). However, the mechanism of interfacial organization of native OB has not yet been fully elucidated, especially

when the objects have been degraded by oxidation, even though such characterization could help understand plant-based beverage reactivity.

The aim of this study was thus to investigate the oxidative behavior of walnut OB using accelerated oxidative storage conditions, to determine the chemical stability of those lipoprotein assemblies when they are in a complex matrix (walnut beverage) or in isolated form at different levels of processing (minimum level, homogenized only, homogenized plus heat-treated). Biophysical tools were used to understand the organization of OB at the interface, and the behavior of their three different constituents, TAG, PL, and proteins (oleosins). Such investigations are required to better understand the reactivity of OB and are of interest for a large panel of food technological applications.

## 2 MATERIALS AND METHODS

All chemicals were purchased from Sigma Aldrich Ltd. (St. Louis, MO), except for ultrapure (UP) water, hexane, and acetic acid purchased from Honeywell Research Chemicals (Charlotte, NC, USA). If not stated otherwise, all biochemical characterizations were conducted at least in triplicate and biophysical characterization at least in duplicate.

### 2.1. Preparation of the complex matrixes and isolation and purification of OB

Walnut kernels (*Juglans regia L., Chandler variety, origin Chile*) were supplied by Sun-Snack AG (St Margrethen, Switzerland). Walnut kernels were soaked in 2% wt. NaCl solution (ratio nuts/solution, 1:20 w/v) and stirred for 16 hours at 200 rpm (Legallais IKA, KS4000 i control) to remove tannins, astringency and soluble impurities in the skin (Ghaderi-Ghahfarrokhi et al., 2017). Sodium azide (0.02% wt.) was added to the final preparation to insure preservation.

#### 2.1.1 Complex matrix preparations: walnut beverages with or without added sodium caseinates (3% wt.)

The procedure for complex matrix preparation was provided by the Institute of Materials Science (Nestlé Research). After soaking and rinsing twice with UP water, 38 g aliquots of walnut kernels were dried, redispersed in 500 mL of UP water and boiled at 90°C in the food processor (Vorwerk Thermomix TM31) for 10 min while blending at low-speed. For one modality of walnut complex matrix including additional emulsifiers, these emulsifiers, i.e. sodium caseinates (3% wt.) were added at this stage. Another modality was produced without sodium caseinates (called hereafter walnut complex matrix). Then, the mixture was blended at maximum power (stage 10). The coarse nut emulsions were pre-homogenized using a high shear laboratory mixer (Silverson, L5M-A) at a shearing speed of 8 000 rpm for 1 min with a

square head. The emulsion was sieved through a 300  $\mu\text{m}$  stainless steel sieve to get rid of large solid particles that could hinder high pressure homogenization. To obtain a fine emulsion with a relatively small particle size, the emulsion was passed through a two-stage laboratory homogenizer (Niro Soavi, Panda 2K) with heads set at  $3.0 \times 10^7$  Pa and  $8.0 \times 10^6$  Pa.

### **2.1.2 Isolation and purification of OB**

OB were isolated from walnut kernels and purified using the method of Kapchie et al. (2011). After soaking and rinsing twice with UP water, the walnut kernels were manually ground with a pestle and mortar. Aliquots (50 g) of walnut kernels were mixed with UP water at ratio of 1:6 (g/mL) and stirred at 10 000 rpm for 5 min in a lab disperser (Ultra-turrax, IKA, T18 digital). The mixture was sieved in 315  $\mu\text{m}$  stainless-steel sieve. The first wash consisted of centrifuging the filtered solution at 4 000 g at 4°C for 30 min (Beckman Coulter, Avanti J-E). The layer of cream at the top of the tube was collected and washed three times in buffer solution (0.1 M Tris-HCl, 4 M sucrose, 0.5 M NaCl, pH 8.6, ratio 1:6 g/mL) by centrifugation at 4 000 g at 4°C for 30 min. The upper phase was collected each time. All the upper phases were pooled, then washed twice in UP water (ratio 1:6 g/mL) by centrifugation at 4 000 g at 4°C for 30 min. The resulting cream layer of isolated OB was dispersed (4% w/v) in a 0.1 M Tris-HCl solution at pH 7. A diagram for the procedure of OB isolation and purification is available in Figure S1 (supplementary material).

### **2.2 Processing of dispersed isolated OB**

High-pressure homogenization (HHP) treatments were carried out in a two-stage high-pressure homogenizer (Niro Soavi, Panda 2K) by applying  $3.0 \times 10^7$  Pa and  $8.0 \times 10^6$  Pa, for first and second head respectively. One fraction of isolated HHP OB was subjected to an additional heat

treatment (modality called hereafter HHPT) at 90°C for 10 min. The minimally processed (MP) sample underwent no processing. In total, three modalities were obtained based on the dispersed OB cream layer solution, named respectively, MP, HHP and HHPT, according to the operation units applied.

## **2.3 Oxidation test challenge to monitor the chemical stability of OB in isolated forms or in complex matrixes**

### **2.3.1 Storage test set-up**

The OB emulsions were divided into 8 mL triplicates in amber centrifuge tubes and stored in an incubator (Legallais IKA KS4000 i control) at 40°C for 20 days under constant agitation at 110 rpm (Genot & Michalski, 2010). Aliquots were taken at days 0, 1, 3, 6, 9, 12, 15 and 20 for analysis of levels of oxidation in the samples (PV and TBARS assays).

### **2.3.2 Monitoring of lipid oxidation using PV and TBARS assays**

Peroxide values (PV) were first determined, using the method of Mihaljević et al. (1996) and Shantha & Decker (1994). This PV index is indicative of the number of active oxygen atoms in the organic chains, leading to the formation of unstable primary oxidation products such as hydroperoxide. 250 µL aliquot of the sample was added to 500 µL of a mixture of methanol and butanol MeOH/BuOH (3:1 v/v) and vortexed for 10 s, and 30 µL of the diluted sample were placed on a clear microplate (ANSI/SLAS (SBS) format) with 230 µL of MeOH/BuOH (3:1 v/v), 2.5 µL of iron chloride solution and 2.5 µL of ammonium thiocyanate. After 10 min of reaction, absorbance was measured at 532 nm using a microplate reader (Nanoquant Infinite 200 Pro, TECAN, Gröedig, Austria). Contribution of protein to PV was eliminated by

comparison with the iodometric normalized method of determination of peroxide index (*Norme Française* NF T60-220, 1968). The results are expressed in meq O<sub>2</sub>/kg of oil.

The thiobarbituric acid reactive substances (TBARS) assay, adapted from Ghani et al. (2017) and Ohkawa et al. (1979), was performed. The TBARS assay measures the equivalent concentration of reactive malondialdehyde (MDA), a secondary oxidation product produced by the degradation of unstable peroxide lipids. 50 µL aliquot of the sample was added to 50 µL of UP water, 200 µL of a solution containing 15% (w/w) of trichloroacetic acid (TCA), 0.375% (w/v) of thiobarbituric acid (TBA) and 0.25 mol/L of hydrochloric acid. The tubes were placed in warm water (90°C) for 15 min, then in ice for 5 min and centrifuged for 10 min at 7 700 g (centrifuge 5427, Eppendorf). Aliquots (200 µL) of the sample were placed on a clear microplate (ANSI/SLAS (SBS)) and absorbance was measured at 532 nm using a microplate reader (Nanoquant Infinite 200 Pro, TECAN, Gröedig, Austria). The results are expressed in mmol equivalent MDA/kg of oil.

#### **2.4 Chemical characterization of walnut kernels**

Walnut kernels (2 g) were ground and incorporated into 5 mL of UP water and 40 mL of Folch solution (chloroform/methanol 2:1 v/v) (Folch, 1957). The mixture was passed through a lab disperser (Ultra-turrax, IKA, T18 digital) for 1 min at between 9 500 and 13 500 rpm. In a 500 mL separating funnel, the solution was washed once with 22.5 mL of NaCl solution at 0.73%, then twice with 50 mL of a solution containing 40 mL of Folch and 10 mL of NaCl solution at 0.58%. The lower phase was collected between each wash and solvents were evaporated under reduced pressure.

#### **2.4.1 Lipid class composition of walnut Folch extracts by thin-layer chromatography (TLC)**

Neutral lipids were separated by one-dimensional migration using hexane/diethylether/acetic acid (65:35:1 v/v/v) in an automatic TLC sampler (Camag, Muttenz, Switzerland) controlled by a Wincats software system (2008) (Bourlieu et al., 2012). After migration, the silica plates were dried at 70°C for 2 min and then revealed with a 15.9% solution of copper sulfate in an orthophosphoric acid/water (92:8 v/v) solution. For each sample, 0.5 mg/mL of lipid solution was used to automatically apply 4 and 8 µL on the thin layer. After revelation, the silica plates were subjected to laser UV detection (Camag TLC scanner 3, Muttenz, Switzerland). The wavelength of maximum absorption was 500 nm, the spots were quantified and spot intensities integrated with Wincats software (2008). Calibration curves were performed with standards of TAG, diacylglycerol (DAG), monoacylglycerol (MAG) and FFA (palmitic, oleic and linoleic acids).

#### **2.4.2 Fatty acid composition of walnut Folch extracts by gas chromatography (GC)**

Fatty acid methyl esters (FAME) were prepared from the walnut Folch extracts (Piombo et al., 2006). Aliquots (5 µL) of methylated Folch extract were analyzed by GC (Focus GC, Thermo Electron Corporation, Massachusetts, USA) equipped with a split injector (ratio of 1/20), a CP-Cil 88 Varian capillary column (50 m × 0.25 mm with a 0.2 µm thick film; Chrompack, Middelburg, The Netherlands) and 1 mL/min of helium as carrier gas. FAME were analyzed using a flame ionization detector and ChromCard Data System (version 2005; Thermo Electron Corporation, Massachusetts, USA).

The column temperature started at 150 °C, increased from 150 °C to 225 °C at a rate of 5°C/min and maintained at 225 °C for 10 min. These chromatographic conditions allowed the correct and rapid separation of all FAME from C10:0 to C24:1. FAME were identified using a mixture of methyl esters as external standard (Mixture ME 100, Larodan, Sweden). The injector and detector temperatures were 250 °C and 270 °C respectively. FA contents are expressed in g per 100 g of fresh product.

#### **2.4.3 Tocopherol content of walnut Folch extracts by high performance liquid chromatography (HPLC)**

HPLC analysis on Folch extracts was performed using the 1290 Agilent System (Massy, France) equipped with a C18 column (250 mm × 4.6 mm i.d., 5 µm, HALO(R)-5 column, AMT, Wilmington, Delaware, USA) and a fluorescence detector, to detect and quantify four distinct tocopherols ( $\alpha$ ,  $\beta$ ,  $\delta$  and  $\gamma$ ) (Moustiés et al., 2019). The mobile phase consisted of ethanol/methanol (40:60 v/v) in isocratic conditions. The temperature of the column was maintained at 25 °C and the flow rate was 0.8 mL/min. Fluorescence detection was set at 296 nm for excitation and 330 nm for emission. The injection volume was 20 µL and the calibration curves were performed with standard solutions from 0.1 to 1.5 mg/L. Each sample was analyzed with three repetitions.

### **2.5 Structural characterization of dispersed isolated OB as their native form or after different physico-chemical treatments during the oxidation challenge**

#### **2.5.1 Droplet size of isolated OB in MP, HHP, and HHPT matrixes**

The size distributions of OB were measured by laser light scattering using a Mastersizer 3000 (Malvern Instruments, Malvern, UK), with two laser sources. The refractive indexes used were

1.333 for water and 1.460 for dispersed OB respectively. The samples were diluted directly in the measurement cell of the apparatus in order to reach 7% obscuration. Several parameters were calculated from the size distribution: the mode diameter, which corresponds to the population of the most frequent OB in the volume distribution, the surface-weighted average diameter of the OB  $d_{32}$  ( $\mu\text{m}$ ), defined as  $\sum n_i d_i^3 / \sum n_i d_i^2$ , and the specific surface area calculated according to the equation  $S = 6 \cdot \phi / d_{32}$  (where  $\phi$  is the volume fraction of lipid in the emulsion).

### **2.5.2 Study of MP, HHP and HHPT matrix microstructure using Confocal Laser Scanning Microscopy (CLSM)**

The matrix microstructure was observed using a CLSM system (Leica SP8, Heidelberg, Germany) on an inverted microscope operated with an argon laser (excitation at 488 nm) and two He-Ne lasers (excitation at 543 and 633 nm) that enabled multi-imaging of a sample by selecting the correct excitation wavelength and filters to collect the light emitted from a given stain. A 64x oil-immersion objective was used for all images. Three fluorescent dyes were used, as already detailed by Bourlieu et al. (2015) to locate i) proteins - Fast Green FCF (6:100 v/v,  $\lambda_{\text{ex}}=633 \text{ nm}$  -  $\lambda_{\text{em}}=655-755 \text{ nm}$ , Invitrogen), ii) non-polar lipids - LipidtoX (0.2:100, v/v,  $\lambda_{\text{ex}}=488 \text{ nm}$  -  $\lambda_{\text{em}}=590 \text{ nm}$ , Invitrogen) and iii) polar lipids - Rd-DOPE (1:100, v/v, 16:0 Liss Rhod PE 1,2-dipalmitoyl-*sn*-glycero-3-phosphoethanolamin-N-(lissamin rhodamin B sulfonyl),  $\lambda_{\text{ex}}=543 \text{ nm}$  -  $\lambda_{\text{em}}=590 \text{ nm}$ , Avanti Polar Lipids). The three dyes were added in a 200  $\mu\text{L}$  aliquots at least 10 min before observation. 10  $\mu\text{L}$  samples were then placed on a glass slide just before observations. The software used for CSLM images was EZ-C1 version 3.40 (Nikon).

### **2.5.3 $\zeta$ -potential measurements of isolated OB in MP, HHP and HHPT matrixes**

The apparent  $\zeta$ -potential of OB in several emulsions diluted at 1:200 v/v in UP water was determined by measuring electrophoretic mobility ( $u$ ) at 25°C using laser Doppler electrophoresis (Nano Z PSS Z300, Nicomp). Measurements were made at 3 mV for 7 min. Henry's law relates  $U$  to the particle  $\zeta$ -potential.

## **2.6 Interfacial behavior of isolated MP OB at the air/water interface**

### **2.6.1 Preparation of model solutions**

To obtain an overview of the different interfacial behaviors of MP OB compounds (TAG, proteins, and PL) several model solutions were prepared based on the proportions of OB constituents in their native form. A solution containing oleosins and TAG (named oleo-TAG) extracted from walnut OB was prepared by introducing 3% wt. oleosins and 95% wt. TAG, diluted to 4% wt. in a solution of 1 M Tris-HCl pH 7. To promote solubilization of the oleosins, TAG were first emulsified in the Tris-HCl solution and then sonicated for 30 s at 1.5 W before the oleosins were incorporated. A second sample containing 3% wt. oleosins and 95% wt. commercial walnut oil (La Tourangelle, France) was also prepared using the same procedure. Another model solution containing L- $\alpha$ -phosphatidylcholine powder from eggPC and commercial walnut oil (named EggPC-WOIL) was prepared by adding 2% wt. of EggPC and 95% wt. of previously emulsified commercial walnut oil, diluted to 4% wt. in a 0.1 M Tris HCl solution at pH 7. Another solution containing 4% wt. of commercial walnut oil diluted in a 0.1 M Tris-HCl solution at pH 7 was also prepared. The model solutions were named respectively oleo-TAG, oleo-WOIL, EggPC-WOIL and WOIL, according to their composition.

### **2.6.2 Ellipsometry and surface pressure measurements**

Experiments were performed using a circular Teflon trough (volume 8 mL, surface area 27 cm<sup>2</sup>). After 5 min of acquisition in UP water to define the zero, the water was replaced by the

4% wt. OB or model sample diluted at a rate of 22.5 mg/L in UP water (1/1600) in the Langmuir trough. The surface pressure (PI, mN/m) and the ellipsometric angle (DELTA, °) were recorded simultaneously at 21.5 °C. The surface pressure was measured according to the Wilhelmy-plate method using a filter paper connected to a microelectronic feedback system to measure the surface pressure (Nima Technology, UK). Values of PI were recorded every 15 s with a precision of  $\pm 0.2$  mN/m. Ellipsometric measurements were carried out with a home-made automated ellipsometer in a “null ellipsometer” configuration (Berge & Renault, 1993; Bourlieu et al., 2020). The laser beam probed a surface of 1 mm<sup>2</sup> and a depth in the order of 1  $\mu$ m and provided insight into the number of molecules at the interface. Values of DELTA were recorded every 15 s with a precision of  $\pm 0.5$  °.

### 2.6.3 Study of interfacial film structures by atomic force microscopy (AFM)

For AFM imaging, interfacial films were transferred onto a freshly-cleaved mica plate using the Langmuir-Blodgett method. The transfer took place at the end of the kinetic adsorption in the Langmuir trough, after the surface pressure of the sample reached a plateau. Barriers were set at a low speed of 10 cm<sup>2</sup>/min and the surface pressure was held constant during the transfer. The mica plate was further observed with an AFM (Multimode Nanoscope 5, Bruker, France) in QNM mode in air (20°C) with standard silicon cantilevers (0.3 N/m), and at a scan rate of 1 Hz. The force was minimized during all scans. To check the integrity of the samples after the different scans and zooms, the same zone was imaged at the end of the analysis. The scanner size was 100×100  $\mu$ m<sup>2</sup>. The processed images were analyzed by the open-source platform Gwyddion.

## 2.7 Statistical analysis

All results are presented as mean  $\pm$  SD. Statistical significance between the OB dispersions was tested by one-way ANOVA. Statistical significance between the two complex matrixes was

tested by t-test. Both tests were conducted using R software (R.2.13.0, <http://cran.r-project.org>).

Statistical Differences between groups were declared significant at  $p < 0.05$ .

Journal Pre-proofs

### 3 RESULTS

#### 3.1 Chemical composition of walnut Folch extract

As expected, lipid class analyses confirmed the presence of TAG, DAG, phytosterols, MAG, PL, and FFA in the walnut kernels. The results identified high concentrations of unsaturated fatty acids (~93% w/w of oil), especially of linoleic acid (LA, C18:2,  $\omega$ 6) (average=  $69.8 \pm 7.4$  % w/w of oil), in a range similar to those found by other authors (Christopoulos & Tsantili, 2015; Maguire et al., 2004). Palmitic acid (C16:0, average=  $6.8 \pm 0.7$  % w/w of oil) was the main saturated fatty acid. In terms of liposoluble vitamins, only vitamin E isomers were detected (average=  $41.0 \pm 20.7$  mg/100g of oil), with a large majority of  $\gamma$ -tocopherols (average=  $36.9 \pm 15.6$  mg/100 g of oil). The total concentrations of fatty acids and the tocopherol contents of OB extracted from walnut are shown Figure S1 (supplementary material).

#### 3.2 Characterization of OB minimally-processed structure and impact on oxidative behavior

CLSM was performed to visualize the microstructure of isolated walnut OB. Selective fluorescent probes were used to locate TAG, PL and proteins. As expected, the structure of OB was in agreement with the model proposed by Huang (1994). Figure 1.A.a. shows OB as a green spherical droplet of TAG surrounded by a red layer of PL embedded in blue proteins. In agreement with the results reported by Gallier et al. (2013), OB ranged in size from 0.5 to 10  $\mu$ m (Fig. 1.A.b.). The  $\zeta$ -potential of the isolated solution was also measured to judge the general physical stability of the emulsion. A moderate absolute value of the  $\zeta$ -potential was evidenced ( $-34.0 \pm 0.6$  mV), providing sufficient negative charge to prevent aggregation or flocculation phenomena.

The oxidative behavior of the minimally processed (MP) isolated OB solution was monitored by measuring the formation of primary (PV) and secondary (TBARS) lipid oxidation products during storage. This test was conducted at neutral pH for a period of 20 days of storage at 40°C. The results are shown in Figure 2.A (MP OB). PV and TBARS did not change much during the first 10 days of storage, pointing a good stability to oxidation phenomenon. After 10 days, the PV concentration began to increase slightly, followed by TBARS after 12 days, due to the transformation of unstable primary products into secondary products. Nevertheless, the change was limited, indicating good stability of OB in their minimally-processed state.

### **3.3 Impact of processing on the structure and oxidative behavior of isolated OB**

The effects of high-pressure homogenization and heat treatment on the structure and oxidative stability of isolated OB were studied (Fig. 2.A - HHP OB, HHPT OB). PV and TBARS of HHP and HHPT OB dispersions increased significantly from the 5<sup>th</sup> day of the test on, revealing lower chemical stability than for MP OB. The oxidation phenomenon was even faster when the OB had undergone an additional heat treatment (HHPT) downstream. In addition, a sensory test (sniffing, n=2) revealed the development of negative off-flavors in the products from the 6<sup>th</sup> day of accelerated storage in the HHPT samples, compared to from the 9<sup>th</sup> and 15<sup>th</sup> day for HHP and MP OB respectively. In terms of structure modification, the CLSM images revealed a reorganization of the membrane of the processed OB, and different impacts depending on the process applied (Fig 1). In the HHP OB sample, fragments of the red and blue layer were missing, indicating membrane damage. In the HHPT OB sample, the membrane was more deteriorated and a blue layer of protein formed, around which objects aggregated. These observations are consistent with the changes in the granulometric profile, in which the largest objects doubled in size (16.4 to 31.1  $\mu\text{m}$ ) in isolated HHP OB compared with HHPT OB (Fig

2). The phenomenon of increasing particle size after homogenization and even more after heat treatment has already been reported in research on walnut OB by Chen et al. (2014). It had also been reported in OB from other sources, such as peanuts, on which Zaaboul et al. (2019) observed severe aggregation and coalescence between OB after HHP followed by sterilization at 95°C for 15 min.

### **3.4 Oxidative behavior of OB in complex matrixes (HHPT walnut beverages with or without added sodium caseinates)**

Two complex HHPT walnut matrixes with or without 3% wt. of sodium caseinates, representative of commercial walnut-based beverages, were prepared to evaluate the impact of additional ingredients in the complex matrix (fibers, walnut proteins, added emulsifiers...) on the oxidative stability of the system. Good chemical stability of complex matrixes was observed in the short term (10 days) Figure 2.B. Both complex matrixes, i.e., with and without sodium caseinates remained quite stable to oxidation even after 20 days, with low oxidation values. More precisely, after 20 days of storage at 40°C, the complex matrix with no sodium caseinates reached a PV value of 4.8 meq O<sub>2</sub>/kg of oil compared to 2.5 meq O<sub>2</sub>/kg of oil in the complex matrix containing sodium caseinates. The TBARS values for the complex matrixes, with and without sodium caseinate(s), were both at 1.4 mmol eq MDA/kg of oil.

Finally, MP OB and HHPT complex matrixes were quite stable to oxidation. Processing isolated OB with HHP or HHPT treatments decrease their stability to oxidation. In comparison, processing walnut complex matrixes (global walnut juice) with or without additional emulsifiers (sodium caseinate) did not induce such oxidative instability.

### 3.5 Behavior of minimally-processed (MP) fresh versus oxidized OB at the air/water interface

Since MP OB seem quite stable to oxidation and can be considered as interesting ingredients for human nutrition, we investigated further their behavior at the air/water interface to gather original data about their behavior when dispersed in an emulsion or foam. Comparison of fresh versus oxidized OB could be helpful to food engineers to detect MP OB degradation in a food system. The interfacial behaviors of fresh and oxidized MP OB solutions ( $PV=30.8 \pm 1.2$  meq  $O_2/kg$  of oil) were characterized using biophysical tools (tensiometry, ellipsometry, atomic force microscopy). Figure 3 summarizes the adsorption kinetics and the AFM images obtained for the two samples at 22.5 mg/L of MP OB. The surface pressure of the fresh MP OB increased from 0 mN/m to approximately 13 mN/m (Fig. 3.A.a.) in less than one minute. After this initial step, the surface pressure continued to increase more progressively for a period of 4.5 hours until it reached a plateau at  $19.8 \pm 0.7$  mN/m. The ellipsometric angle followed a similar pattern until it reached a final value of  $9 \pm 0.5^\circ$ , illustrating the rise of matter at the interface due to the amphiphilic nature of OB. In contrast, in the oxidized MP OB solution diluted at 22.5 mg/L, the final surface pressure and ellipsometric angle were respectively  $15 \pm 0.8$  mN/m and  $5.1 \pm 0.5^\circ$ , lower than those in the fresh MP OB solution. This points to a different organization of the particles at the interface as well as the formation of a thinner monolayer in the case of oxidized OB.

After 4.5 h of stabilization of tensiometry and ellipsometry signals, a Langmuir-Blodgett transfer of the interfacial film was performed and imaged using AFM. The resulting images Figure 3.b. provide information on the interfacial reorganization of OB objects in fresh and oxidized MP OB samples. A background with height variation of 0.6 nm was observed in the

image of the fresh MP OB (Fig. 3.A.b.), with the presence of evenly spread generally large protuberances of different lateral sizes and 4 nm in height. Bright "peaks" of 6-8 nm were observed at the center of some protuberances. Smaller bright domains, around 1.5-2 nm in height, were also visible. These smaller domains were not spherical but mainly had edges. The AFM image of oxidized MP OB emulsion (Fig. 3.B.b) shows a different interfacial organization, with the same background as that of the fresh MP OB solution, but with no protuberances.

To better understand the interfacial structure of MP OB observed in AFM images, a RhoPE dye was incorporated in the MP OB sample to locate the PL in the interfacial film using fluorescence microscopy. The images of the fluorescent sample observed with CLSM (fig. 4.a) showed that the layer was heterogenous, with continuous fluorescence (RhoPE) in the background, indicating the presence of PL (in red). The AFM images were then recorded on the most homogenous parts (Fig. 4.b). The AFM images of MP OB with and without the RhoPE were similar, indicating that the fluorescent probes do not affect the interfacial organization of the sample. In addition, as described in the followed section, model solutions were prepared to identify precisely the other components in the interfacial films.

### **3.6 Behaviors of model solutions at the air/water interface**

When OB rise to the air/water interface, they are likely to open and the competing interactions of their three different components will then determine the physical configuration of the interface: TAG, PL, oleosins but also, probably, some still intact OB. To elucidate the mechanism of organization at the air/water interface, model samples were prepared. These models were initially formulated at 4% wt. of lipid in Tris-HCl solution at pH 7, before being diluted at 22.5 mg/L in UP water. We first compared two model solutions. The first one was

formulated with oleosins and TAG, prepared using the same ratio as that found in natural OB (3% wt. oleosins, 95% wt. TAG or commercial walnut oil). The second model solution was only composed by commercial walnut oil (95% wt). In the AFM images of oleo-TAG (Fig. 5.A) and oleo-WOIL (Fig. 5.B), bright “peaks” 4 to 8 nm in height and irregularly shaped domains 1.5-2 nm in height were visible, similar to those present in the AFM image of the MP OB sample. However, the “peaks” did not appear in the WOIL sample (Fig. 5.C), in which irregular protuberances between 2 and 6 nm in height were observed, in addition to domains 1 nm in height, which we assumed to be gel-phase TAG. To complete these observations, the EggPC-WOIL sample containing 2% wt. of EggPC and 95% wt. of commercial walnut oil, was then compared to the WOIL sample. The ellipsometric angle of the EggPC-WOIL sample reached a higher value of  $6.3^\circ$  after 4.5 h, compared to  $5.2^\circ$  for the WOIL sample, reflecting the greater thickness of the interfacial film. The AFM image of the EggPC-WOIL sample (Fig. 5.D) showed a denser background material, with homogeneous protuberances 6 nm in height, compared to the AFM images of the WOIL sample (Fig. 5.C).

## 4 DISCUSSION

### 4.1 The good chemical stability of walnut OB is evidenced in both processed complex matrixes and in minimally-processed isolated form

Despite the limited physical stability of walnut beverages (Y. Chen et al., 2014), the results of storage test under accelerated oxidation conditions highlighted the good chemical stability of these plant-based beverages, thus increasing their interest for food applications. The remarkable stability to oxidation of the processed complex matrixes can be explained by the presence of endogenous proteins that form a second protective layer around OB. Additionally, large quantities of AO compounds such as  $\gamma$ -tocopherols, but also various phenolic compounds (polyphenols, phenolic acids such as gallic, ellagic, and flavonoids) as described by Zhang et al. (2009), help delay the oxidation phenomenon.

In the complex matrix with added sodium caseinates, we could have expected an enhancement of stability linked to the addition of this emulsifier. Indeed, Haahr & Jacobsen (2008), who evaluated the effect of several types of emulsifiers - including sodium caseinates - on the oxidative stability of 10% wt. oil in water emulsions containing  $\omega$ 3 rich fish oil, demonstrated an antioxidant (AO) effect of sodium caseinates. In their study, the emulsion stabilized by sodium caseinates was shown to oxidize more slowly than the emulsion stabilized with Tween 80, despite the much more negative  $\zeta$ -potential of sodium caseinates at pH 7. The difference in oxidative stability was associated with the ability of sodium caseinates to chelate iron (Sugiarto et al., 2010) and to form a 10-nm-thick layer at the surface of dispersed oil droplet, thus protecting unsaturated FA from oxidation (Hu et al., 2003). In our study, sodium caseinates did not appear to provide significant additional oxidative stability to the walnut complex matrix, suggesting that the system is already relatively stable with respect to oxidation.

Similarly, to processed walnut complex matrixes, MP OB exhibited good chemical stability over the first 10 days of storage, thanks to their native structure and fat-soluble AO content. The limited difference in the concentration of oxidation products indicates that isolating OB did not affect their protection capacity against oxidation, underlining the interest of using these minimally-processed compounds in food applications. Similar results were obtained on soybean OB by Kapchie et al. (2013), who found low oxidation of isolated OB suspensions without the presence of prooxidant metal species at physiological pH and after 12 days of storage at 60°C, while the PV was 14 meq O<sub>2</sub>/kg and TBARS was 0.4 mmol eq MDA/kg. Ding et al. (2018) also studied the chemical stability of isolated OB dispersions for 14 days in the dark at room temperature. Their results confirmed the good stability to oxidation of the emulsions, with low PV and TBARS of 7 meq O<sub>2</sub>/kg and 0.003 mmol eq MDA/kg respectively after 14 days.

#### **4.2. Processed OB (HHP and HHPT) were less stable to oxidation than MP OB**

The processing operations, i.e. homogenization and heat-treatment, resulted in the reorganization of the OB membrane, increasing exchanges with reactive species. This change in the membrane led to a significant increase in oxidation compared to MP OB, despite the similar chemical composition of the systems. These results confirm the importance of the native assembly in the chemical stability of OB, underlining the need to rethink food processing to insure better preservation of natural assemblies and their properties when these assemblies are used in quite purified forms.

Overall, the oxidation of these MP OB reduced the internal cohesion of the OB and consequently also that of its components, leading to a different interfacial organization.

#### **4.3. The adsorption mechanism of isolated MP OB was determined at the air/water interface and differ from the one proposed for soybean OB**

The combination of simultaneous ellipsometry, tensiometry and AFM results of MP OB and model solutions made it possible to examine the behavior of minimally-processed walnut OB at the air/water interface. Overall, biophysical results indicate that isolated fresh MP OB retained their native microstructure when adsorbed to the air/water interface. The model solutions containing oleosins (3% wt.) led us attribute the 6-12 nm height “peaks” on the fresh OB AFM images to the presence of oleosins. Indeed, a height of 12 nm was determined for soybean oleosins by Zielbauer et al. (2018) using small angle neutron scattering, which correspond to the height of the “peaks” obtained in AFM size profiles. Big bright protuberances 4 nm in height visible on the AFM images of MP OB were identified as oleosins, PL and TAG assemblies, that remained very cohesive due to hydrophobic interactions.

In contrast, the structural modification of the membrane caused by oxidation reduce cohesion between the different components, as revealed by the results of the biophysical analysis. The final ellipsometric angle and surface pressure were indeed lower than in the fresh MP OB sample. The AFM images reinforced these results, showing a different interfacial organization when the objects were oxidized, in particular the absence of TAG, PL and oleosins assemblies. Smaller domains (1 nm in height) were probably lipid domains in crystalline phase, composed of palmitic and stearic saturated FA. This observation tends to confirm the thermotropic crystalline mesophase of OB membrane proposed by Nikiforidis (2019) and suggests that oxidation led to the solubilization of oxidized unsaturated TAG and PL.

Waschatko, Schiedt, et al., (2012) proposed different models for the structural organization of soybean OB interface. Figure 6.A presents a model for the organization of walnut OB at

interfaces based on the models of Waschatko et al., emphasizing the new understanding enabled by the results we obtained in the present study. When the isolated fresh OB solution is deposited in the Langmuir trough, OB rise to the interface before opening. When the lateral surface pressure is sufficient to maintain cohesion of the components, they remain assembled and form protuberances, visible at the interface, with the central hydrophobic domain of oleosin oriented toward the surface. In addition, mixtures of unsaturated and saturated fats can form fat droplets, as confirmed by the presence of irregularly shaped globules in the AFM images of isolated fresh MP OB. Low height domains of saturated TAG and PL complete the interface background. When the membrane structure is altered by protein cleavage (Waschatko et al., 2012) or by oxidation, the lateral pressure is no longer sufficient to maintain the assemblies of oleosins, TAG and PL, as illustrated in the model proposed in Figure 6.B. The rigid native "T" conformation of oleosins is no longer preserved, and some oleosins are presumed to unfold at the interface or are solubilized as protein-lipid clusters. Like in the fresh sample, saturated PL and TAG domains also form at the interface, but oxidation is responsible for the solubilization of unsaturated lipids, leading to the disappearance of fat globule in the AFM images of the oxidized sample.

This better understanding of the interfacial behavior of MP OB from different botanical sources will ease the development of innovative emulsions or foams in which MP OB can be used as functional ingredients. They will be specifically useful to design heterogeneous systems in which OB will be used as emulsifiers.

## CONCLUSIONS

Oxidation tests and biophysical tools were used to study the oxidative and interfacial behavior of walnut OB in different matrixes. Strong chemical stability of the complex walnut matrixes was evidenced under accelerated oxidation conditions, thanks to the presence of many endogenous proteins and antioxidant compounds. Isolation of OB from the complex matrix did not alter their protection against oxidation, thanks to their native assembly as well their fat-soluble antioxidant content. Nevertheless, processing of OB accelerated their chemical oxidation.

The organizational mechanism at the air/water interface of walnut MP OB is demonstrated. When MP OB adsorb at an air/water interface, the good cohesive ability of their native assembly allows them to keep intact their microstructure. Oxidation was shown to alter this internal cohesion of OB by structural modification of the membrane.

Taken together, our results show that when OB are incorporated in the structure of new food products, their chemical and physical stability during the design process should be taken into consideration. Indeed, alteration of the physical structure of OB during processing may affect their chemical stability during storage and hence the quality of the final product expected by the consumer. This finding underlines the need to rethink food processing to preserve natural assemblies and their beneficial properties.

**Declaration of Competing Interest**

The authors declare that they have no known competing financial interests or personal relationships that could have appeared to influence the work reported in this paper.

**Acknowledgments**

The authors acknowledge Carine Alcon and the imaging facility MRI (*Montpellier Ressources Imagerie*, Montpellier, France), member of the national infrastructure France-BioImaging infrastructure supported by the French National Research Agency (ANR-10-INBS-04, «Investments for the future»). We also would like to thank the MRic platform (*Microscopy Rennes Imaging Center*, Rennes, France) for technical assistance with the confocal laser scanning microscope. Finally, the 2CBioMIF platform (ScanMAT-UMS 2001, Rennes, France) is acknowledged for allowing the biophysical characterization of the samples presented in this article.

C. Bourlieu, V. Vié and J. Kergomard were responsible for the design and the content of the manuscript. All the authors participated in the experimental design, the collection, the interpretation of data. J. Kergomard wrote the manuscript and all the authors were involved in reviewing and correcting the manuscript. All the authors approved submission of the final article.

**References**

- Barre, A., Simplicien, M., Cassan, G., Benoist, H., & Rougé, P. (2018). Oil bodies (oleosomes) : Occurrence, structure, allergenicity. *Revue Française d'Allergologie*, 58(8), 574-580. <https://doi.org/10.1016/j.reval.2018.10.005>
- Berge, B., & Renault, A. (1993). Ellipsometry Study of 2D Crystallization of 1-Alcohol Monolayers at the Water Surface. *Europhysics Letters (EPL)*, 21(7), 773-777. <https://doi.org/10.1209/0295-5075/21/7/010>
- Bettini, S., Santino, A., Giancane, G., & Valli, L. (2014). Reconstituted oil bodies characterization at the air/water and at the air/oil/water interfaces. *Colloids and Surfaces B: Biointerfaces*, 122, 12-18. <https://doi.org/10.1016/j.colsurfb.2014.06.044>
- Bourlieu, C., Mahdoueni, W., Paboeuf, G., Gicquel, E., Ménard, O., Pezennec, S., Bouhallab, S., Deglaire, A., Dupont, D., Carrière, F., & Vié, V. (2020). Physico-chemical behaviors of human and bovine milk membrane extracts and their influence on gastric lipase adsorption. *Biochimie*, 169, 95-105. <https://doi.org/10.1016/j.biochi.2019.12.003>
- Bourlieu, C., Ménard, O., De La Chevasnerie, A., Sams, L., Rousseau, F., Madec, M.-N., Robert, B., Deglaire, A., Pezennec, S., Bouhallab, S., Carrière, F., & Dupont, D. (2015). The structure of infant formulas impacts their lipolysis, proteolysis and disintegration during in vitro gastric digestion. *Food Chemistry*, 182, 224-235. <https://doi.org/10.1016/j.foodchem.2015.03.001>
- Bourlieu, C., Rousseau, F., Briard-Bion, V., Madec, M.-N., & Bouhallab, S. (2012). Hydrolysis of native milk fat globules by microbial lipases : Mechanisms and

- modulation of interfacial quality. *Food Research International*, 49(1), 533-544.  
<https://doi.org/10.1016/j.foodres.2012.07.036>
- Chen, B., McClements, D. J., Gray, D. A., & Decker, E. A. (2012). Physical and oxidative stability of pre-emulsified oil bodies extracted from soybeans. *Food Chemistry*, 132(3), 1514-1520. <https://doi.org/10.1016/j.foodchem.2011.11.144>
- Chen, Y., Lu, Y., Yu, A., Kong, X., & Hua, Y. (2014). Stable Mixed Beverage is Produced from Walnut Milk and Raw Soymilk by Homogenization with Subsequent Heating. *Food Science and Technology Research*, 20(3), 583-591.  
<https://doi.org/10.3136/fstr.20.583>
- Christopoulos, M. V., & Tsantili, E. (2015). Oil composition in stored walnut cultivars—Quality and nutritional value. *European Journal of Lipid Science and Technology*, 117(3), 338-348. <https://doi.org/10.1002/ejlt.201400082>
- De Chirico, S., di Bari, V., Romero Guzmán, M. J., Nikiforidis, C. V., Foster, T., & Gray, D. (2020). Assessment of rapeseed oil body (oleosome) lipolytic activity as an effective predictor of emulsion purity and stability. *Food Chemistry*, 316, 126355.  
<https://doi.org/10.1016/j.foodchem.2020.126355>
- Ding, J., Xu, Z., Qi, B., Jiang, L., & Sui, X. (2018). Physicochemical and oxidative stability of a soybean oleosome-based emulsion and its in vitro digestive fate as affected by (-)-epigallocatechin-3-gallate. *Food & Function*, 9(12), 6146-6154.  
<https://doi.org/10.1039/C8FO01215F>
- Folch, J. (1957). A Simple Method for the Isolation and Purification of Total Lipids from Animal Tissues. *J Biol Chem*, 226, 497-509.

- Frandsen, G. I., Mundy, J., & Tzen, J. T. C. (2001). Oil bodies and their associated proteins, oleosin and caleosin. *Physiologia Plantarum*, *112*(3), 301-307.  
<https://doi.org/10.1034/j.1399-3054.2001.1120301.x>
- Gallier, S., Tate, H., & Singh, H. (2013). In Vitro Gastric and Intestinal Digestion of a Walnut Oil Body Dispersion. *Journal of Agricultural and Food Chemistry*, *61*(2), 410-417.  
<https://doi.org/10.1021/jf303456a>
- Genot, C., & Michalski, M.-C. (2010). Impact métabolique des structures et de l'oxydation des lipides dans les aliments. *Innovations Agronomiques (10)*, 43-67. (2010).  
<http://agris.fao.org/agris-search/search.do?recordID=LV2016008646>
- Ghaderi-Ghahfarrokhi, M., Sadeghi-Mahoonak, A. R., Alami, M., & Mousavi Khanegah, A. (2017). Effect of processing treatments on polyphenol removal from kernel of two Iranian acorns varieties. *International Food Research Journal*, *24*(1), 86-93.
- Ghani, M. A., Barril, C., Bedgood, D. R., & Prenzler, P. D. (2017). Measurement of antioxidant activity with the thiobarbituric acid reactive substances assay. *Food Chemistry*, *230*, 195-207. <https://doi.org/10.1016/j.foodchem.2017.02.127>
- Haahr, A.-M., & Jacobsen, C. (2008). Emulsifier type, metal chelation and pH affect oxidative stability of n-3-enriched emulsions. *European Journal of Lipid Science and Technology*, *110*(10), 949-961. <https://doi.org/10.1002/ejlt.200800035>
- Hayes, D., Angove, M. J., Tucci, J., & Dennis, C. (2016). Walnuts (*Juglans regia*) Chemical Composition and Research in Human Health. *Critical Reviews in Food Science and Nutrition*, *56*(8), 1231-1241. <https://doi.org/10.1080/10408398.2012.760516>
- Huang, A. H. C. (1994). Structure of plant seed oil bodies. *Current Opinion in Structural Biology*, *4*(4), 493-498. [https://doi.org/10.1016/S0959-440X\(94\)90210-0](https://doi.org/10.1016/S0959-440X(94)90210-0)

- Kapchie, V. N., Hauck, C. C., Wang, H., & Murphy, P. A. (2011). Process Improvement for Semipurified Oleosomes on a Pilot-Plant Scale. *Journal of Food Science*, *76*(6), C853-C860. <https://doi.org/10.1111/j.1750-3841.2011.02278.x>
- Kapchie, V. N., Yao, L., Hauck, C. C., Wang, T., & Murphy, P. A. (2013). Oxidative stability of soybean oil in oleosomes as affected by pH and iron. *Food Chemistry*, *141*(3), 2286-2293. <https://doi.org/10.1016/j.foodchem.2013.05.018>
- Khor, V. K., Shen, W.-J., & Kraemer, F. B. (2013). Lipid Droplet Metabolism. *Current opinion in clinical nutrition and metabolic care*, *16*(6), 632-637. <https://doi.org/10.1097/MCO.0b013e3283651106>
- Maguire, L. S., O'Sullivan, S. M., Galvin, K., O'Connor, T. P., & O'Brien, N. M. (2004). Fatty acid profile, tocopherol, squalene and phytosterol content of walnuts, almonds, peanuts, hazelnuts and the macadamia nut. *International Journal of Food Sciences and Nutrition*, *55*(3), 171-178. <https://doi.org/10.1080/09637480410001725175>
- Mihaljević, B., Katušin-Ražem, B., & Ražem, D. (1996). The reevaluation of the ferric thiocyanate assay for lipid hydroperoxides with special considerations of the mechanistic aspects of the response. *Free Radical Biology and Medicine*, *21*(1), 53-63. [https://doi.org/10.1016/0891-5849\(95\)02224-4](https://doi.org/10.1016/0891-5849(95)02224-4)
- Miraliakbari, H., & Shahidi, F. (2008). Lipid Class Compositions, Tocopherols and Sterols of Tree Nut Oils Extracted with Different Solvents. *Journal of Food Lipids*, *15*(1), 81-96. <https://doi.org/10.1111/j.1745-4522.2007.00104.x>
- Moustiés, C., Bourlieu, C., Barea, B., Servent, A., Alter, P., Lebrun, M., Hemery, Y. M., Laillou, A., & Avallone, S. (2019). Lipid Composition and State of Oxidation of Fortified Infant Flours in Low-Income Countries Are Not Optimal and Strongly

- Affected by the Time of Storage. *European Journal of Lipid Science and Technology*, 121(11), 1900173. <https://doi.org/10.1002/ejlt.201900173>
- Napier, J. A., Beaudoin, F., Tatham, A. S., Alexander, L. G., & Shewry, P. R. (2001). The seed oleosins : Structure, properties and biological role. In *Advances in Botanical Research* (Vol. 35, p. 111-138). Academic Press. [https://doi.org/10.1016/S0065-2296\(01\)35005-X](https://doi.org/10.1016/S0065-2296(01)35005-X)
- Nikiforidis, C. V. (2019). Structure and functions of oleosomes (oil bodies). *Advances in Colloid and Interface Science*, 274, 102039. <https://doi.org/10.1016/j.cis.2019.102039>
- Nikiforidis, C. V., Matsakidou, A., & Kiosseoglou, V. (2014). Composition, properties and potential food applications of natural emulsions and cream materials based on oil bodies. *RSC Advances*, 4(48), 25067-25078. <https://doi.org/10.1039/C4RA00903G>
- Nuchi, C. D., Hernandez, P., McClements, D. J., & Decker, E. A. (2002). Ability of lipid hydroperoxides to partition into surfactant micelles and alter lipid oxidation rates in emulsions. *Journal of Agricultural and Food Chemistry*, 50(19), 5445-5449. <https://doi.org/10.1021/jf020095j>
- Ohkawa, H., Ohishi, N., & Yagi, K. (1979). Assay for lipid peroxides in animal tissues by thiobarbituric acid reaction. *Analytical Biochemistry*, 95(2), 351-358. [https://doi.org/10.1016/0003-2697\(79\)90738-3](https://doi.org/10.1016/0003-2697(79)90738-3)
- Piombo, G., Barouh, N., Barea, B., Boulanger, R., Brat, P., Pina, M., & Villeneuve, P. (2006). Characterization of the seed oils from kiwi (*Actinidia chinensis*), passion fruit (*Passiflora edulis*) and guava (*Psidium guajava*). *Oléagineux, Corps Gras, Lipides*, 13(2-3), 195-199. <https://doi.org/10.1051/ocl.2006.0026>

- Samdani, G. K., McClements, D. J., & Decker, E. A. (2018). Impact of Phospholipids and Tocopherols on the Oxidative Stability of Soybean Oil-in-Water Emulsions. *Journal of Agricultural and Food Chemistry*, 66(15), 3939-3948.  
<https://doi.org/10.1021/acs.jafc.8b00677>
- Shantha, N. C., & Decker, E. A. (1994). Rapid, Sensitive, Iron-Based Spectrophotometric Methods for Determination of Peroxide Values of Food Lipids. *Journal of AOAC INTERNATIONAL*, 77(2), 421-424. <https://doi.org/10.1093/jaoac/77.2.421>
- Shimada, T. L., Hayashi, M., & Hara-Nishimura, I. (2018). Membrane Dynamics and Multiple Functions of Oil Bodies in Seeds and Leaves. *Plant Physiology*, 176(1), 199-207. <https://doi.org/10.1104/pp.17.01522>
- Simopoulos, A. P. (2002). The importance of the ratio of omega-6/omega-3 essential fatty acids. *Biomedicine & Pharmacotherapy = Biomedecine & Pharmacotherapie*, 56(8), 365-379. [https://doi.org/10.1016/s0753-3322\(02\)00253-6](https://doi.org/10.1016/s0753-3322(02)00253-6)
- Tzen, J., Cao, Y., Laurent, P., Ratnayake, C., & Huang, A. (1993). Lipids, Proteins, and Structure of Seed Oil Bodies from Diverse Species. *Plant Physiology*, 101(1), 267-276. <https://doi.org/10.1104/pp.101.1.267>
- Venkatachalam, M., & Sathe, S. K. (2006). Chemical composition of selected edible nut seeds. *Journal of Agricultural and Food Chemistry*, 54(13), 4705-4714.  
<https://doi.org/10.1021/jf0606959>
- Villière, A. (2005). *Approche physico-chimique et sensorielle de l'oxydation des lipides dans des émulsions stabilisées par des protéines* [These de doctorat, Nantes].  
<https://www.theses.fr/2005NANT2042>

- Walther, T. C., & Farese, R. V. (2012). Lipid Droplets and Cellular Lipid Metabolism. *Annual Review of Biochemistry*, *81*(1), 687-714. <https://doi.org/10.1146/annurev-biochem-061009-102430>
- Waschatko, G., Schiedt, B., Vilgis, T. A., & Junghans, A. (2012). Soybean Oleosomes Behavior at the Air–Water Interface. *The Journal of Physical Chemistry B*, *116*(35), 10832-10841. <https://doi.org/10.1021/jp211871v>
- White, D. A., Fisk, I. D., Mitchell, J. R., Wolf, B., Hill, S. E., & Gray, D. A. (2008). Sunflower-seed oil body emulsions : Rheology and stability assessment of a natural emulsion. *Food Hydrocolloids*, *22*(7), 1224-1232. <https://doi.org/10.1016/j.foodhyd.2007.07.004>
- Zaaboul, F., Raza, H., Cao, C., & Yuanfa, L. (2019). The impact of roasting, high pressure homogenization and sterilization on peanut milk and its oil bodies. *Food Chemistry*, *280*, 270-277. <https://doi.org/10.1016/j.foodchem.2018.12.047>
- Zhang, Z., Liao, L., Moore, J., Wu, T., & Wang, Z. (2009). Antioxidant phenolic compounds from walnut kernels (*Juglans regia* L.). *Food Chemistry*, *113*(1), 160-165. <https://doi.org/10.1016/j.foodchem.2008.07.061>
- Zhao, L., Chen, Y., Yan, Z., Kong, X., & Hua, Y. (2016). Physicochemical and rheological properties and oxidative stability of oil bodies recovered from soybean aqueous extract at different pHs. *Food Hydrocolloids*, *61*, 685-694. <https://doi.org/10.1016/j.foodhyd.2016.06.032>
- Zielbauer, B. I., Jackson, A. J., Maurer, S., Waschatko, G., Ghebremedhin, M., Rogers, S. E., Heenan, R. K., Porcar, L., & Vilgis, T. A. (2018). Soybean oleosomes studied by

small angle neutron scattering (SANS). *Journal of Colloid and Interface Science*, 529, 197-204. <https://doi.org/10.1016/j.jcis.2018.05.080>

## FIGURES

Figure captions.

**Figure 1** a) Optical microscopy, b) particle size distribution and c) confocal laser scanning microscopy (red dye: PL, blue dye: proteins, green dye: TAG) of isolated OB emulsions having undergone different treatment(s). (A) MP OB b) trimodal, modes: 7.64  $\mu\text{m}$ , 0.675  $\mu\text{m}$ , 2.13  $\mu\text{m}$ ; (B) HHP OB b) bimodal, modes: 16.4  $\mu\text{m}$ , 0.523  $\mu\text{m}$ ; and (C) HHPT OB b) bimodal, modes: 31.1  $\mu\text{m}$ , 0.523  $\mu\text{m}$ .

**Figure 2** a) PV and b) TBARS values during 20 days at 40°C and 110 rpm of (A) processed isolated walnut OB (MP, HHP, HHPT); and (B) walnut complex matrixes with and without 3% wt. of sodium caseinates. Data shown are average of three replicates.

**Figure 3** a) Evolution of surface pressure (red circles; PI, mN/m) and ellipsometric angle (blue triangle; DELTA, °) during the 4.5 hours experiments of adsorption on air-water interface and

b) monolayer AFM images ( $10 \times 10 \mu\text{m}^2$ ) and size profiles after 4.5 hours experiments of isolated solution of (A) Fresh MP OB ( $\text{PI}_f=20.3 \text{ mN/m}$ ;  $\text{DELTA}_f=9.2^\circ$ ) and (B) Oxidized MP OB ( $\text{PI}_f=14.7 \text{ mN/m}$ ;  $\text{DELTA}_f=5.1^\circ$ ) diluted in UP water at 22.5 mg/L.

**Figure 4** a) Confocal Laser Scanning Microscopy ( $448 \times 448 \mu\text{m}^2$  and  $184 \times 184 \mu\text{m}^2$ ) and b) Atomic force microscopy images ( $25 \times 25 \mu\text{m}^2$  and  $5 \times 5 \mu\text{m}^2$ ) of monolayer of MP OB isolated solution diluted at 22.5 mg/L in UP water dyed with Rhodamine PE.

**Figure 5** AFM images ( $5 \times 5 \mu\text{m}^2$  and  $1 \times 1 \mu\text{m}^2$ ) of Langmuir-Blodgett films of 22.5 mg/L of a) oleo-TAG; b) Oleo-WOIL; c) WOIL; and d) EggPC-WOIL after 4.5 hours of acquisition. Final values of surface pressure (PI, mN/m) and ellipsometric angle (DELTA, °) were recorded at 4.5 hours of acquisition when the films were transferred on mica plate.

**Figure 6** Proposed mechanisms of OB organization at the air-water interface for (A) Fresh MP OB; and (B) Oxidized MP OB.

Figure 1

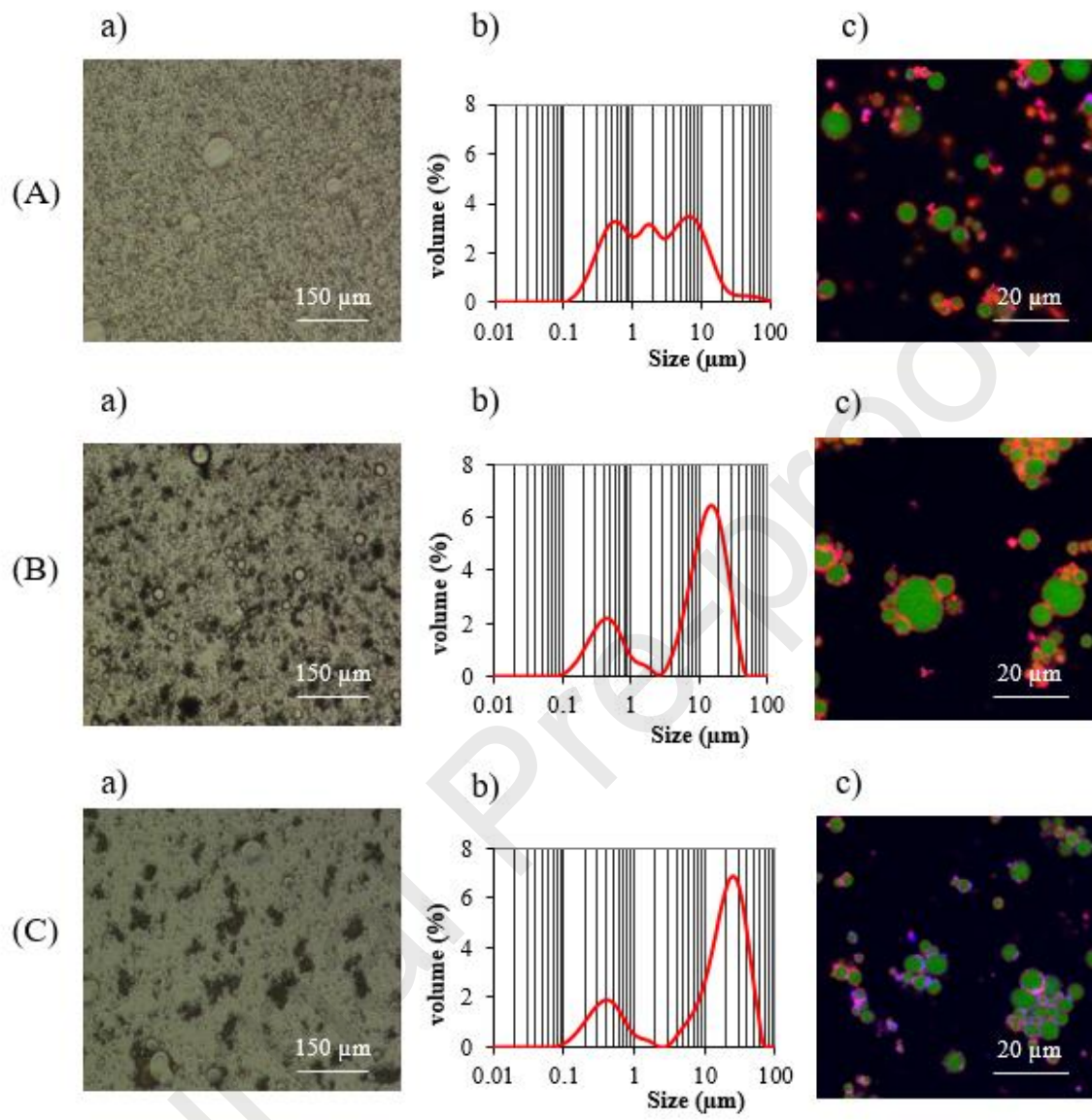


Figure 2

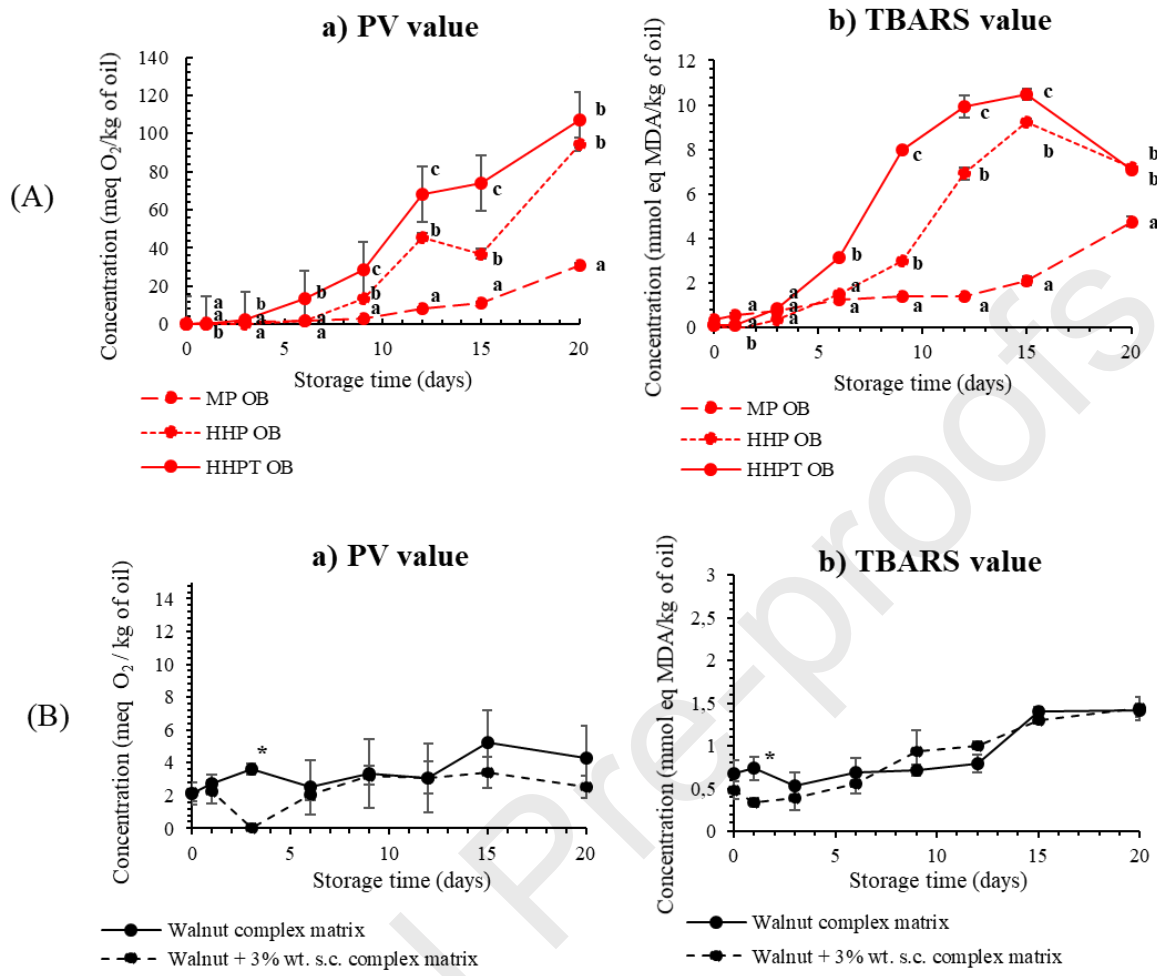
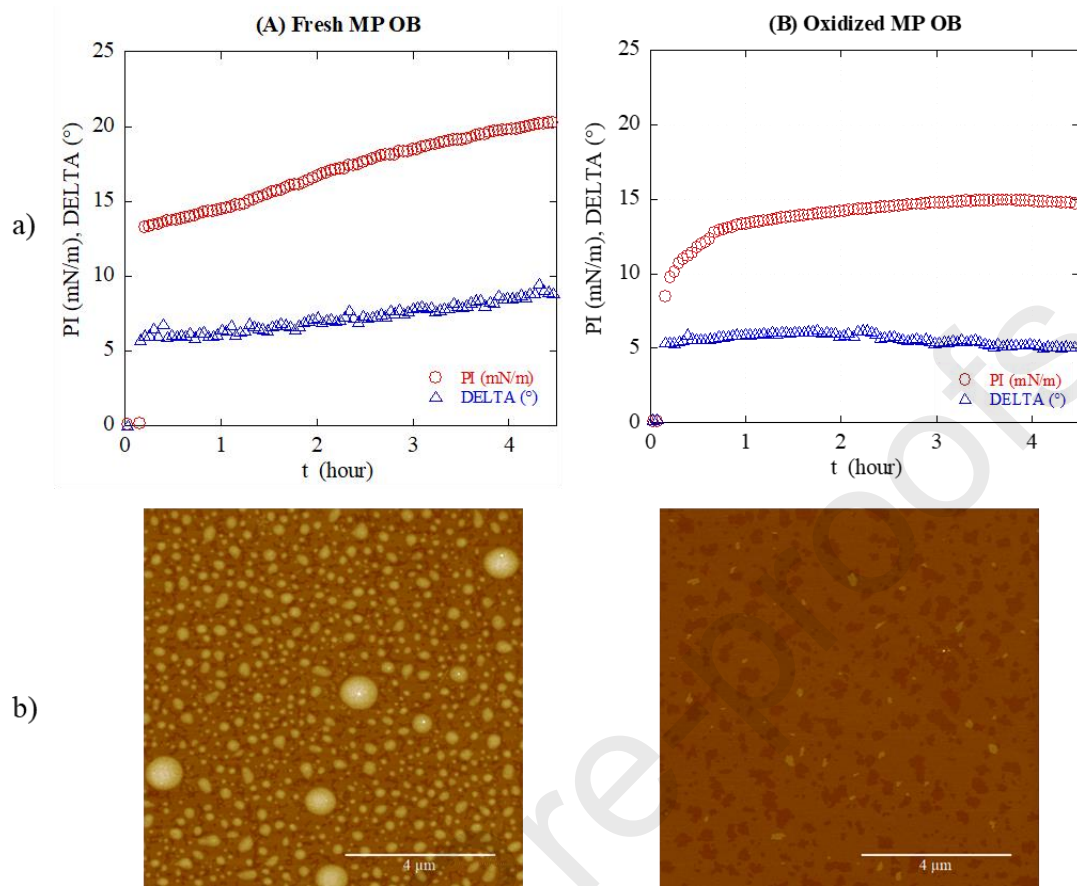


Figure 3



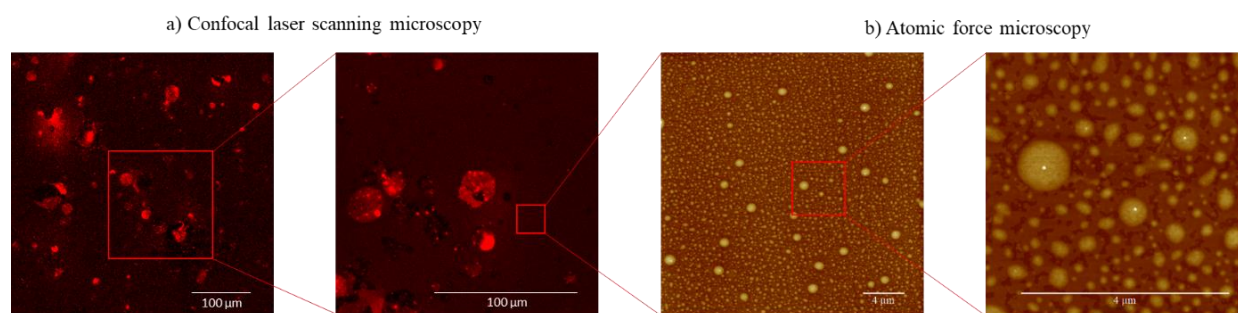
**Figure 4**

Figure 5

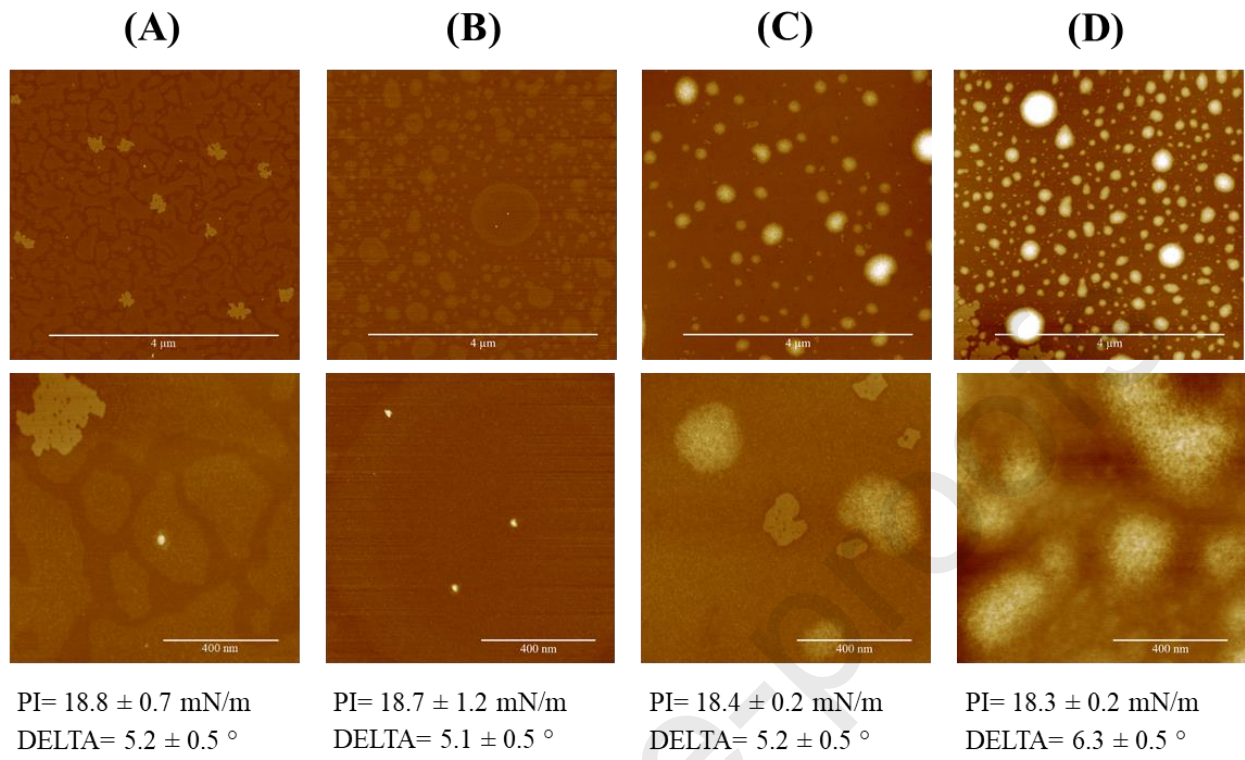
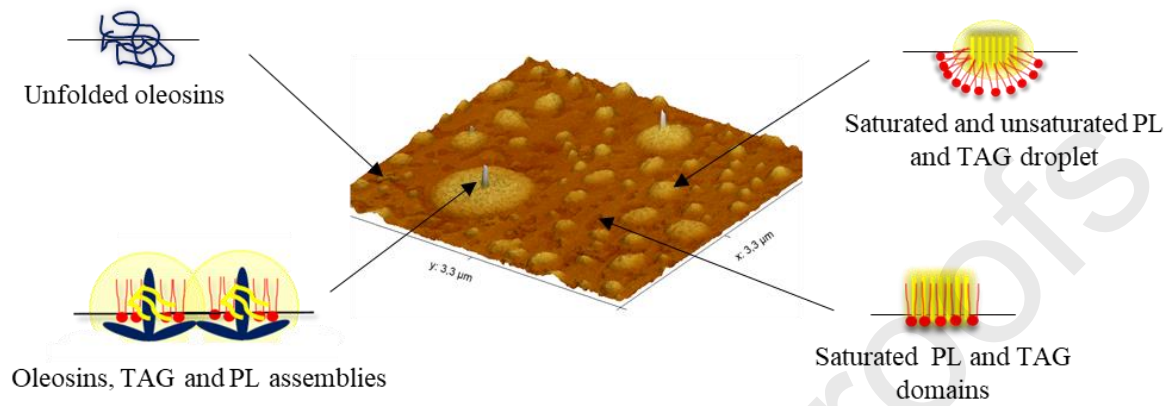
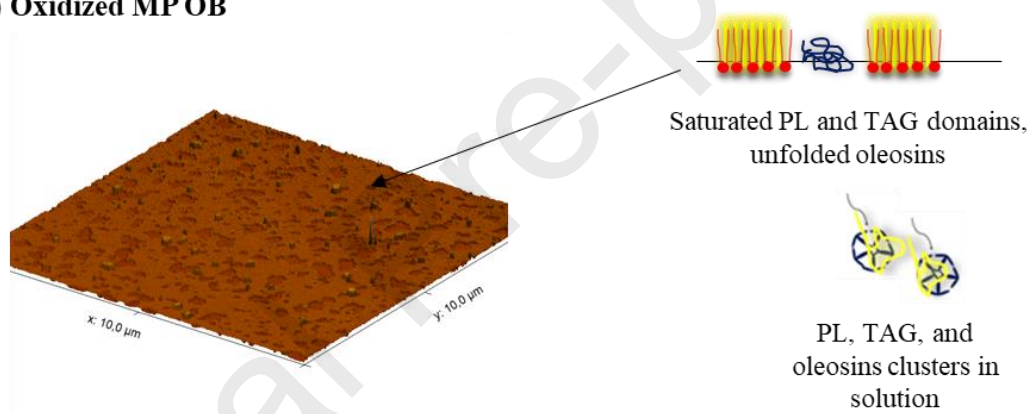


Figure 6

## (A) Fresh MP OB



## (B) Oxidized MP OB



**Declaration of interests**

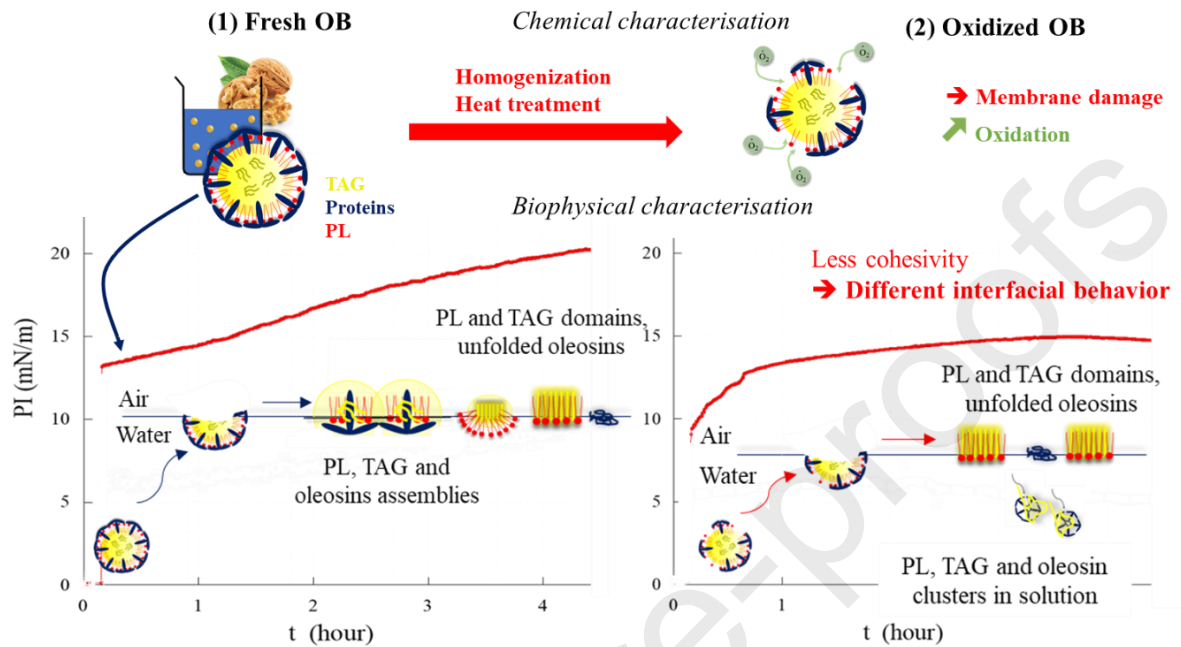
The authors declare that they have no known competing financial interests or personal relationships that could have appeared to influence the work reported in this paper.

The authors declare the following financial interests/personal relationships which may be considered as potential competing interests:

**Credit Author Statement**

C. Bourlieu, V. Vié and J. Kergomard were responsible for the design and the content of the manuscript. All the authors participated in the experimental design, the collection, the interpretation of data. J. Kergomard wrote the manuscript and all the authors were involved in reviewing and correcting the manuscript. All the authors approved submission of the final article.

## Graphical abstract



## HIGHLIGHTS

- Walnut complex matrix exhibited strong chemical stability against oxidation
- The chemical stability was preserved when OB were isolated from the complex matrix
- Processing operation altered the OB membrane, decreasing the chemical stability

- The OB microstructure remained intact during adsorption at an air/water interface
- Oxidation altered the internal cohesion of OB and thus the interfacial organization

Journal Pre-proofs